Clays and Clay Minerals, Vol. 42, No. 3, 259–268, 1994.

SUPERGENE VERMICULITIZATION OF PHLOGOPITE AND BIOTITE IN ULTRAMAFIC AND MAFIC ROCKS, CENTRAL KOREA

HI-SOO MOON,[1] YUNGOO SONG,[1] AND S. Y. LEE[2]

[1] Department of Geology, Yonsei University, 134 Shinchon-dong, Seodaemun-ku, Seoul 120-749, Korea

[2] Environmental Sciences Division, Oak Ridge National Laboratory, P.O. Box 2008, Oak Ridge, Tennessee 37831, U.S.A.

Abstract—An X-ray diffraction study of vermiculitized micas in ultramafic and mafic intrusive rocks from Cheongyang, Korea, shows the following weathering sequence: mica → ordered mica/vermiculite interstratification → vermiculite. Electron microprobe analyses show the general trends of K leaching and Ca enrichment with increased weathering. The vermiculitization of phlogopite from ultramafic rocks proceeds by means of a continuous decrease in Al-for-Si tetrahedral substitutions and a progressive increase in Al-for-(Fe^{2+} + Mg) octahedral substitutions in the early stage of weathering. These substitutions occur to compensate for the excess of negative charge in the mica-like layer, in agreement with currently accepted vermiculitization mechanisms. They change to a slight increase of Al-for-Si tetrahedral substitutions in the late stage of the vermiculitization of phlogopite, owing to the oxidation of Fe despite its low content. However, the behavior of Fe in the late stage of the transformation of biotite into vermiculite is significantly different; that is, Fe increases substantially. The reason for this Fe increase in the late stage remains unresolved. Recalculations of the structural formulas on the basis of several assumptions indicate that the oxidation of Fe is necessary for the vermiculite derived from biotite to form the reasonable structural formulas.

Key Words—Biotite, Interstratification, Phlogopite, Vermiculitization, Weathering.

INTRODUCTION

Trioctahedral micas in basic igneous rocks are not stable under earth-surface conditions. They weather rapidly in alteration zones, mainly by progressive hydration of interlayer cations. Many workers have studied this process by observing both naturally weathered micaceous minerals and mica altered artificially in the laboratory. Supergene vermiculitization of trioctahedral micas through intermediate stages of interstratified mica/vermiculite has been identified as one of the main mineral weathering sequences reported in the literature (Coleman *et al.*, 1963; Rhoades and Coleman, 1967; Meunier and Velde, 1979; April *et al.*, 1986; Ildefonse *et al.*, 1986; Banfield and Eggleton, 1988; Bain *et al.*, 1990; Fordham, 1990a). Vermiculite deposits at Cheongyang, South Korea, appear to be derived from both phlogopite in ultramafic and biotite in mafic intrusive rocks (Song *et al.*, 1990). This paper 1) describes the mineralogical and chemical changes during the pronounced vermiculitization undergone by phlogopite and biotite in different parent materials as weathering progresses and 2) shows the compositional differences between vermiculites derived from phlogopite and biotite.

MATERIALS AND METHODS

Vermiculite samples were collected from weathered ultramafic and mafic intrusive rocks showing typical weathering profiles in the Cheongyang area, Chungchungnam-do, central Korea (Figure 1). Ultramafic rock, which mainly consists of phlogopite and a relatively small amount of clinopyroxene, tremolite, magnetite, and chromite, is usually covered by soil (saprolite) ranging from 0.3 to 1 m in depth. The soils have well-defined weathering profiles. Five samples (P-1 to P-5) were systematically collected from the saprolite weathered from the ultramafic rock (Figure 2). One fresh (B-10) and nine slightly weathered mafic rock samples (B-1 to B-9) were randomly collected from the surface in a quarry (at B site in Figure 1) located southwest of the phlogopite sampling area. This mafic rock intrudes the ultramafic rock and contains biotite, hornblende, clinopyroxene, quartz, and a small amount of garnet and plagioclase. The slightly weathered samples contain vermiculites, which exhibit different degrees of weathering and vermiculitization.

Polished thin sections of the altered rock samples were made for petrographic and subsequent electron microprobe examination after epoxy resin impregnation. The clay size fractions (<2 μm) were separated from the weathered rock for X-ray diffraction (XRD) analysis using ultrasonic treatment. No chemical pretreatments were employed.

Phlogopite, biotite, and other minerals were analyzed with a JEOL JCXA-733 WDS model electron microprobe. A beam current of 1.5×10^{-8} A, a 10 μm beam diameter, and an 80 s counting time were used. Data were corrected using the method of Bence and Albee (1968). To minimize errors associated with mo-

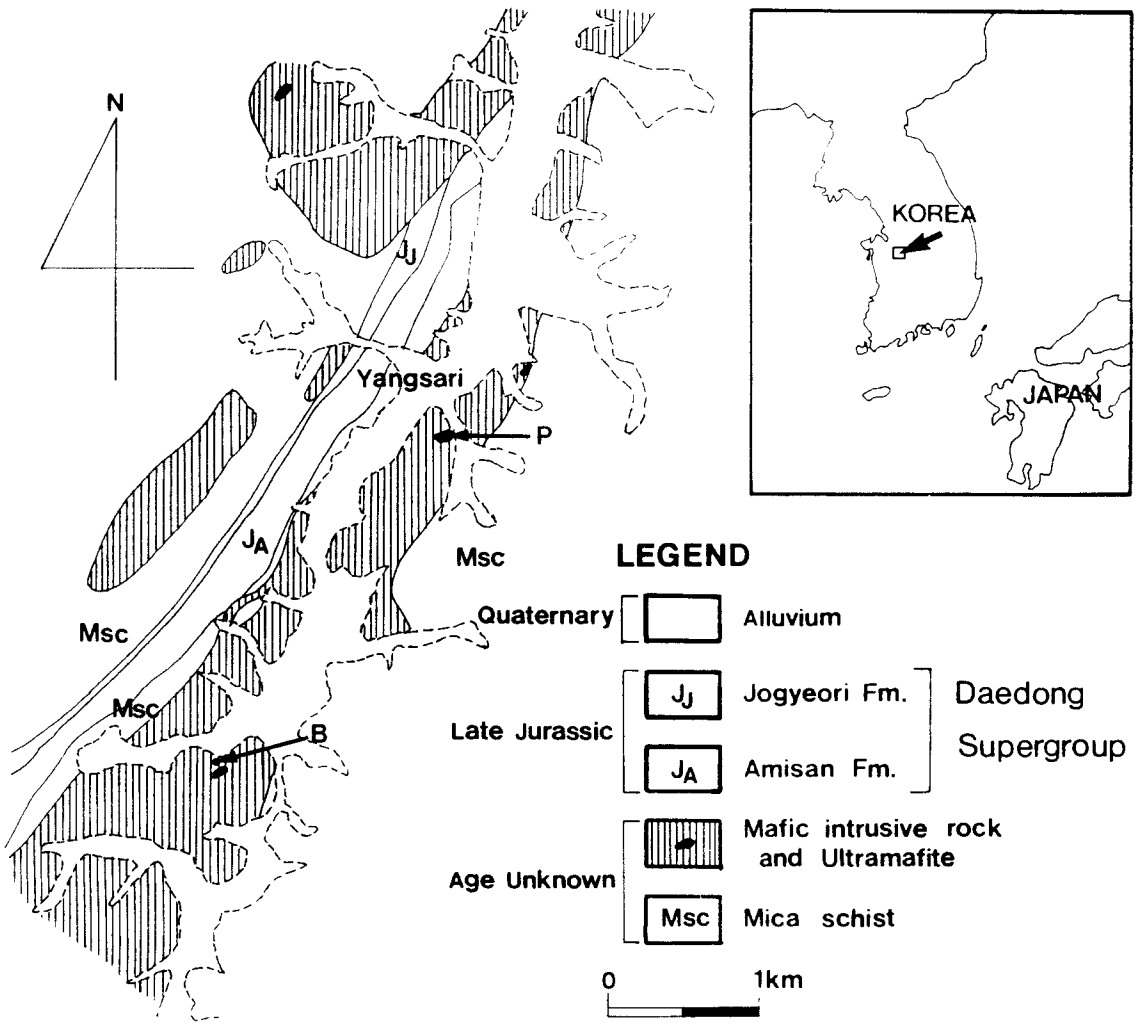

Figure 1. Simplified geological map of the Cheongyang area, Korea, showing sampling sites. "P" represents the sampling site for phlogopite and its altered products (P-1 to P-5); "B", the site for biotite and its altered products (B-1 to B-10).

bilization under the beam, K and Na were measured first. Well-characterized minerals were used for the standard materials: diopside for Si and Ca, almandine for Al and Fe, rutile for Ti, chromite for Cr, olivine for Mg, rhodonite for Mn, albite or Na, sanidine for K, and pure nickel oxide for Ni. The error limit (1 sigma) for Si is 1% and the limits for Al, Fe, Mg, Ti, K, and Ca are 1% to 2%. The Kiss (1967) method was used to analyze ferrous Fe contents of the purified clay size fraction (<2 μm) separated from weathered ultramafic rocks. A Ca-saturated sample was prepared for the clay size fraction (<2 μm) of sample P-1 to determine the actual octahedral Mg contents. A 1 N calcium chloride ($CaCl_2$) solution was mixed with the sample, the clay suspension was centrifuged, and the clear supernatant liquid was decanted. This procedure was repeated four times with fresh solution. the sample was then washed with deionized water and centrifuged until the decanted solution no longer showed the presence of chloride. The degree of saturation was confirmed by XRD.

XRD traces were obtained from untreated, Mg-saturated, ethylene glycol-treated, and heat-treated oriented aggregates as well as random bulk rock powders through the use of a MAC MXP-3 XRD system with Ni-filtered Cu-Kα radiation, divergent and receiving slits of 1 mm and 0.15 mm, respectively.

The semiquantitative abundances of clay and nonclay minerals from selected bulk samples of weathering profiles of ultramafic rock were determined by the method of MacKenzie (1958) on the basis of XRD analyses and bulk chemical analyses. For the semiquantitative analysis, the chemical data for bulk samples (P-1 to P-5) and chemical composition of each

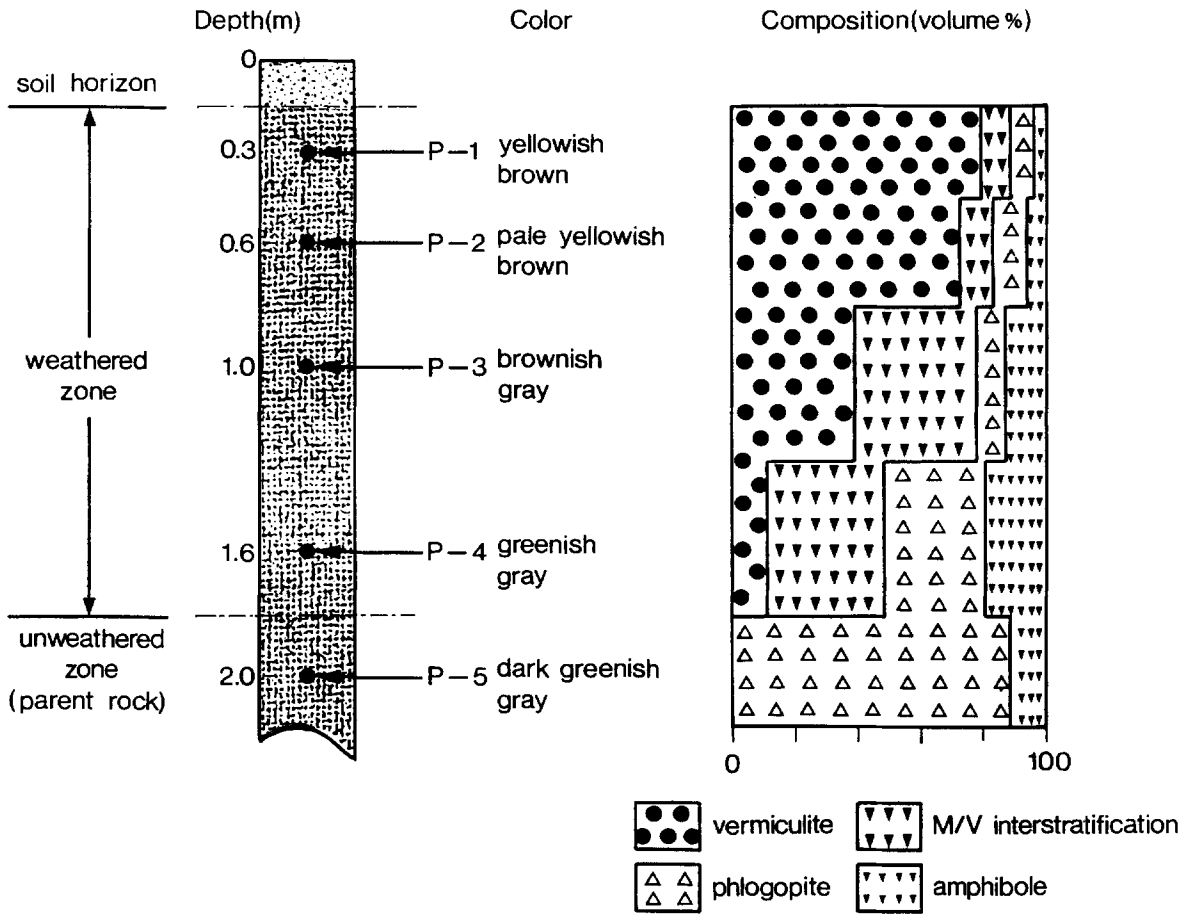

Figure 2. Columnar section showing sample horizons of weathering profiles developed in ultramafic rocks as shown in Figure 1.

mineral were used in accordance with the methods reported earlier by Kim (1992) and Song *et al.* (1990), respectively.

RESULTS AND DISCUSSION

Mineralogical characterization

Representative XRD traces of whole rock samples are shown in Figure 3. They illustrate that the dominant clay mineral assemblage in all samples from two different parent rocks consists of vermiculite (14.5 Å) and interstratified mica/vermiculite (24.5 Å and 12.7 Å), except for P-5 and B-10 as shown in Figure 3. XRD traces of P-5 and B-10 in Figure 3 represent mineralogy of unweathered ultramafic and mafic rock in this area, which contains chiefly mica (phlogopite and biotite) with small amounts of amphibole. Other accessory minerals such as clinopyroxene and opaque minerals (magnetite and chromite) often cannot be identified by XRD, but those minerals are easily identified by petrographic study.

All <2 μm size fractions from weathered ultramafic and mafic rock samples gave sharp peaks at 14.5 Å and moderately broad diffraction peaks at 7.4 Å and 4.9 Å (Figure 4). These peaks are not significantly affected by ethylene glycol solvation after Mg saturation, but they collapse to 9.9 Å at 550°C, which indicates the presence of vermiculite. Before Mg saturation, relatively broad XRD peaks were observed at 25.2–25.5 Å and 12.5–12.7 Å in many of the <2 μm size fractions of the samples. These peaks indicate the presence of a regularly interstratified mica/vermiculite (M/V). In addition, a weak 14.5 Å peak from the vermiculite and the original 10 Å mica peak seen in bulk XRD patterns were also depicted (Figure 3). There was no evidence of the presence of hydroxyaluminum interlayered vermiculite in the samples. The ordered M/V is indicated by a rational series of 00ℓ spacings with a periodicity of 25.2 Å in oriented aggregates. The best-resolved patterns (sample P-3 and B-3) approached the calculated XRD pattern obtained by the method of Reynolds (1980) for regularly interstratified M/V with R =

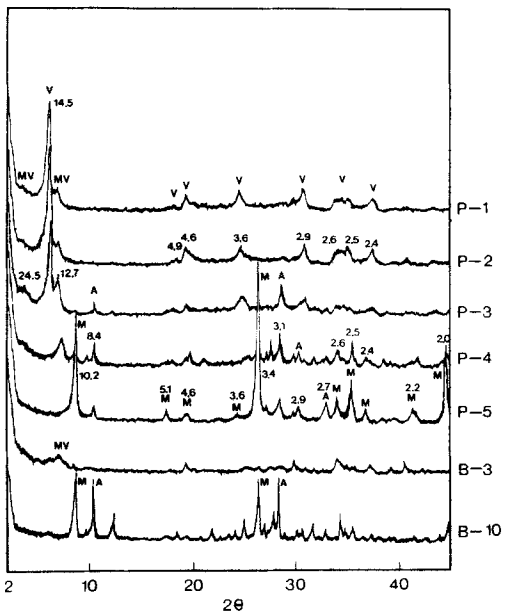

Figure 3. X-ray diffraction patterns of representative bulk samples collected at P (P-1 to P-5) and B (B-3 and B-10) sites as shown in Figures 1 and 2 (CuKα). V = vermiculite, MV = mica/vermiculite interstratification, M = mica, and A = amphibole. Numbers by peaks are in angstroms (Å).

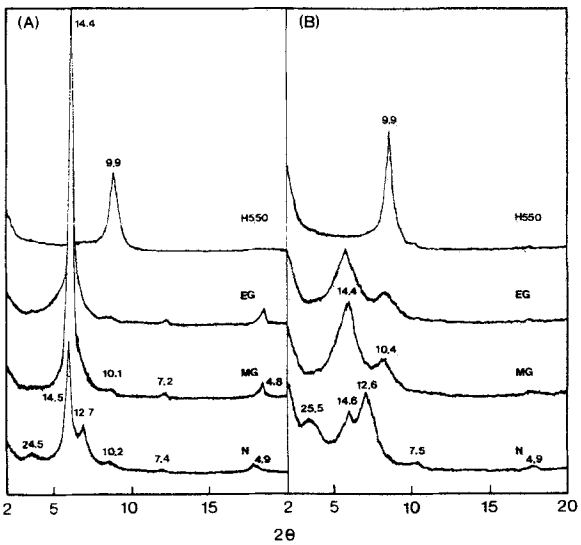

Figure 4. X-ray diffraction patterns of oriented, Mg-saturated, ethylene-glycolated, and heat-treated for some representative samples of <2 μm size fractions of vermiculite: A) vermiculite derived from phlogopite (P-3) and B) vermiculite derived from biotite (B-3). N = untreated, MG = Mg-saturated, EG = ethylene glycol saturated, and H550 = heated to 550°C. Numbers by peaks are angstroms (Å).

1 and with 50% vermiculite layers (Song *et al.*, 1990). The 060 reflections at 1.53–1.55 Å confirmed the trioctahedral character of the mica and vermiculite (not shown here).

As presented in the right column of Figure 2, the lower part of the weathered zone (P-4) has abundant M/V mixed-layered material. And its relative abundance decreases in the upper part of the weathering profile. There is a continuous decrease in phlogopite abundance and an increase in vermiculite content from the bottom to the top of the weathering profile. These results clearly suggest that vermiculites are the product of the weathering of phlogopite and biotite, which have originated from ultramafic and mafic intrusive rocks, respectively. The weathering process thus appears to be mica (phlogopite and biotite) → interstratified M/V → vermiculite.

General chemical characterization

Representative electron microprobe analyses of the phlogopite (P-5) and biotite (B-10) and their weathering products (P-1 to P-4 and B-1 to B-9) are listed in Tables 1 and 2 with their structural formulas. The structural formulas were calculated on the basis of 22 oxygens on the assumption that the octahedral sites were completely occupied. If the sum of octahedral cations exceeded 6, the excess Mg contents were treated as interlayer cations. Ferrous Fe contents for phlogopite and its altered products were determined by the Kiss (1967) method, and average values are listed in Table 1. Ferrous Fe contents for biotite and its altered products were not determined because the purified samples contained a significant amount of impurities. All Fe in biotite and altered products of the biotite was assumed to be in the ferrous state. The analytical result of Ca-saturated vermiculite (P-lCa) is also listed in Table 1. This result agrees well with the published data of Newman and Brown (1987).

Unaltered phlogopite (P-5 in Table 1) is characterized by a large amount of K (10.03 wt. %) and a relatively high ferrous Fe content (4.50 wt. %) in comparison with the K and ferrous Fe levels of altered products (P-1 to P-4). The both unaltered and altered phlogopite contain a significant amount of Cr (0.4–0.6 wt. %) except for vermiculite (P-1 and B-1 in Tables 1 and 2), which is considered to be an interstratification of M/V. Data for phlogopite and altered products (Table 1) show the common variational trends of K leaching and Ca enrichment with increasing vermiculitization (from P-5 to P-1). Biotite (B-10 in Table 2) is characterized by a larger amount of Fe and relatively smaller amounts of Si and Mg than those of phlogopite. The distinct enrichment of Na and Fe and the release of Si and Ti as weathering increases are general trends in biotite and its altered products (e.g., Fordham, 1990a, 1990b, 1990c; Ildefonse *et al.*, 1986). These can be observed in Table 2 from B-10 to B-1, except for Na. Slight enrichment of Na can be recognized in the beginning of alteration. Data for biotite and altered prod-

Table 1. Electron microprobe analyses and structural formulae for phlogopite and their altered products from the ultramafic rock as shown in Figure 2 (in average values).

	P-1 (22)[1]	P-2 (25)	P-3 (20)	P-4 (18)	P-5 (24)	P-1Ca[2] (15)
	← Increase of alteration →					
SiO_2	40.72	40.44	40.35	41.20	41.36	40.05
TiO_2	0.64	0.71	0.71	0.65	0.70	0.79
Cr_2O_3	0.60	0.59	0.44	0.45	0.49	0.61
Al_2O_3	12.28	11.72	11.21	11.64	11.85	12.43
Fe_2O_3	5.51	5.53	5.09	3.81	1.79	6.17
FeO	0.33	0.55	0.78	2.96	4.50	0.37
MnO	0.05	0.06	0.03	0.08	0.05	0.05
MgO	23.56	22.90	22.90	22.34	22.51	21.64
NiO	0.14	0.14	0.14	0.14	0.13	0.10
CaO	1.44	1.09	1.06	0.65	0.06	4.55
Na_2O	0.01	0.12	0.07	0.09	0.05	0.03
K_2O	0.20	2.14	2.66	7.42	10.03	0.53
Total	85.49	86.00	85.45	91.43	93.52	87.83
	Number of cations on the basis of 22 oxygens					
Si	6.04	6.05	6.09	6.03	6.01	6.00
Al(IV)	1.96	1.95	1.91	1.97	1.99	2.00
Al(VI)	0.19	0.12	0.09	0.04	0.04	0.14
Ti	0.07	0.08	0.08	0.07	0.08	0.08
Cr	0.07	0.07	0.05	0.05	0.06	0.07
Fe^{3+}	0.62	0.62	0.58	0.42	0.20	0.68
Fe^{2+}	0.04	0.07	0.10	0.36	0.55	0.05
Mn	0.01	0.01	0.00	0.01	0.01	0.01
Ni	0.02	0.02	0.02	0.02	0.02	0.01
Mg	4.98	5.01	5.08	4.87	4.88	4.71
Σ(VI)	6.00	6.00	6.00	5.84	5.84	5.75
Mg[3]	0.23	0.08	0.07	0.00	0.00	0.00
Ca	0.23	0.18	0.17	0.10	0.01	0.71
Na	0.00	0.04	0.02	0.02	0.01	0.01
K	0.04	0.41	0.51	1.39	1.86	0.01
Σ(interlayer cations)	0.50	0.71	0.77	1.51	1.88	0.73

[1] Numbers indicate the number of analyzed points.
[2] Data for Ca-saturated P-1 sample (vermiculite).
[3] Mg treated as interlayer cations assuming that the octahedral sites were to be completely occupied.

ucts (Table 2) also show the variational trend of K leaching but a less distinct trend of Ca enrichment with increasing vermiculitization (from B-10 to B-1).

Substitutions of Si, Al, Fe, and Mg in mica-like layers

Vermiculitization of micas results in an increase of positive charge or a decrease of net negative charge in mica-like layers. Factors causing a decrease of negative charge can be considered as follows: 1) oxidation of ferrous Fe in octahedral sites, 2) substitution of Si for Al in tetrahedral sites, and 3) increase in the number of cations in octahedral sites. Changes in the number of atoms in various structural sites are depicted in Figures 5 and 6. Mg contents in interlayer cations plotted in Figure 5D are calculated from Table 1 on the assumption that there are 0.2 vacancies per unit cell in octahedral sites on the basis of microprobe data for phlogopite published by Newman and Brown (1987). The variations of Al(IV) (tetrahedral Al), Al(VI) (octahedral Al), Fe^{2+}, Fe^{3+}, and Mg contents from phlogopite to vermiculite show clear trends of compositional change in the early stage, i.e., Al(VI), Fe^{3+}, and total Mg increase; Al(IV), Fe^{2+}, and (Fe^{2+} + Fe^{3+}) decrease; and octahedral Mg remains nearly constant with increasing vermiculitization (Figures 5A–5D). The standard deviation of Al(IV) was 0.035 for P-1, 0.032 for P-2, 0.023 for P-3, 0.040 for P-4, and 0.027 for P-5. Considering the standard deviation of the chemical analyses, these variational trends are clearly different.

The significant mineralogical changes, as shown in Figures 2 and 3, induced by these chemical changes are a continuous slight decrease of the Al-for-Si tetrahedral substitutions together with a general increase in the Al-for-(Fe^{2+} + Mg) octahedral substitutions with increased weathering (Figure 5C and 5D). The dramatic increase of Fe^{3+} in spite of a decrease of (Fe^{2+} + Fe^{3+}) strongly indicates the oxidation of Fe^{2+} to Fe^{3+} (Figure 5C). In the late stage of the vermiculitization of phlogopite, these trends are slightly changed

Table 2. Electron microprobe analyses and structural formulae for biotite and their altered products from mafic intrusive rock.

	B-1	B-2	B-3	B-4	B-5	B-6	B-7	B-8	B-9	B-10
	← Increase of alteration →									
SiO_2	29.83	30.15	29.75	33.33	33.16	34.67	36.04	35.66	36.77	36.44
TiO_2	0.16	0.07	0.13	0.08	0.14	2.75	2.13	2.90	2.98	3.02
Al_2O_3	18.70	18.77	18.12	17.61	18.89	13.39	13.86	13.71	13.94	13.09
FeO[1]	23.87	23.65	22.78	18.60	20.88	20.91	19.74	20.17	18.68	18.90
MnO	0.18	0.20	0.18	0.13	0.16	0.08	0.13	0.17	0.13	0.16
MgO	9.20	9.91	10.74	9.82	8.89	8.97	9.91	10.01	9.53	11.80
CaO	0.69	0.57	0.52	0.69	0.86	0.89	0.81	0.51	0.61	0.00
Na_2O	0.07	0.14	0.12	0.24	0.13	0.11	0.27	0.54	0.20	0.11
K_2O	0.48	0.61	0.70	0.74	0.58	4.62	5.23	6.00	7.91	9.45
Total	83.18	84.07	83.04	81.30	83.04	86.39	88.12	89.67	90.75	92.97
	Number of cations on the basis of 22 oxygens									
Si	5.13	5.12	5.11	5.65	5.52	5.78	5.85	5.74	5.84	5.72
Al(IV)	2.87	2.88	2.89	2.35	2.48	2.22	2.15	2.26	2.16	2.28
Al(VI)	0.92	0.88	0.78	1.17	1.22	0.40	0.50	0.34	0.45	0.14
Ti	0.02	0.01	0.02	0.01	0.02	0.34	0.26	0.35	0.36	0.36
Fe[2]	3.43	3.36	3.27	2.64	2.91	2.91	2.68	2.71	2.48	2.48
Mn	0.03	0.03	0.03	0.02	0.02	0.01	0.02	0.02	0.02	0.02
Mg	1.60	1.72	1.90	2.16	1.83	2.23	2.40	2.40	2.26	2.76
Σ(VI)	6.00	6.00	6.00	6.00	6.00	5.89	5.86	5.82	5.57	5.76
Mg[3]	0.76	0.79	0.86	0.32	0.37	0.00	0.00	0.00	0.00	0.00
Ca	0.13	0.10	0.10	0.13	0.15	0.16	0.14	0.09	0.10	0.00
Na	0.02	0.05	0.04	0.08	0.04	0.04	0.09	0.17	0.06	0.03
K	0.11	0.13	0.15	0.16	0.12	0.98	1.08	1.23	1.60	1.89
Σ(interlayer cation)	1.02	1.07	1.15	0.69	0.68	1.18	1.31	1.49	1.76	1.92

[1] Biotite data (B-10) obtained from the sample occurred in fresh intrusive mafic rock.
[2] Total Fe treated as ferrous.
[3] Mg treated as interlayer cations assuming that the octahedral sites were to be completely occupied.

by an increase of Al(IV) and Al(T) (total Al) (Figure 5B). These results are probably due to charge compensation, as K release during vermiculitization of phlogopite affects the layer charge balance. The associated enrichment of Ca and Mg is not sufficient to compensate for the excess negative charge. These processes appear to require changes in the 2:1 layer of altered materials to compensate for the excess of negative charge. The slight decrease of tetrahedral Al-for-Si substitutions and the increase of octahedral Al-for-(Fe^{2+} + Mg) substitutions in the early stage (see P-5 to P-3 in Table 1 and Figure 5A) are considered spontaneous change for the excess of negative charge to balance as weathering advances. These changes agree well with the increasing dioctahedral character of the clay minerals as weathering advances (Proust *et al.*, 1986; Fordham, 1990b, 1990c). Different trends, however, are observed in the late stages of vermiculitization of phlogopite, showing a slight increase of tetrahedral Al-for-Si substitutions. In this case, Fe oxidation is also necessary to compensate for part of the excess negative charge in spite of the small amount of total Fe in the phlogopite. The surplus of positive charge due to the oxidation causes an increase of Al-for-Si tetrahedral substitution.

Compositional changes mentioned above are more distinct in the vermiculitization of biotite (Figures 6A–6D). The early stage is the weathering of biotite into interstratified phases in which the vermiculitization of biotite produces variational trends similar to those of phlogopite in the early stages. In the late stage of the vermiculitization of biotite, interstratified phases alter to vermiculite, where Mg contents decrease and Al(T) contents increase constantly, Al(IV) and Fe contents increase substantially, and Al(VI) contents are nearly constant. Assuming that all Fe is treated as ferric in the vermiculitic phase, the Fe contents also increase significantly. the chief structural changes induced by these chemical changes are a distinct increase of the tetrahedral Al-for-Si substitutions together with the remains and/or a slight decrease of the octahedral Al-for-(Fe + Mg) substitutions, in spite of an increase of Al(T) with increased weathering.

Two controlling factors can be inferred concerning the change of the late stage in the vermiculitization of biotite: 1) the increase of Fe and Al in structural units and 2) the oxidation of ferrous Fe in octahedral sites. The increase of Fe and Al contribute to an excess of positive charges in 2:1 layers. The oxidation of ferrous Fe significantly affects the increase in total positive

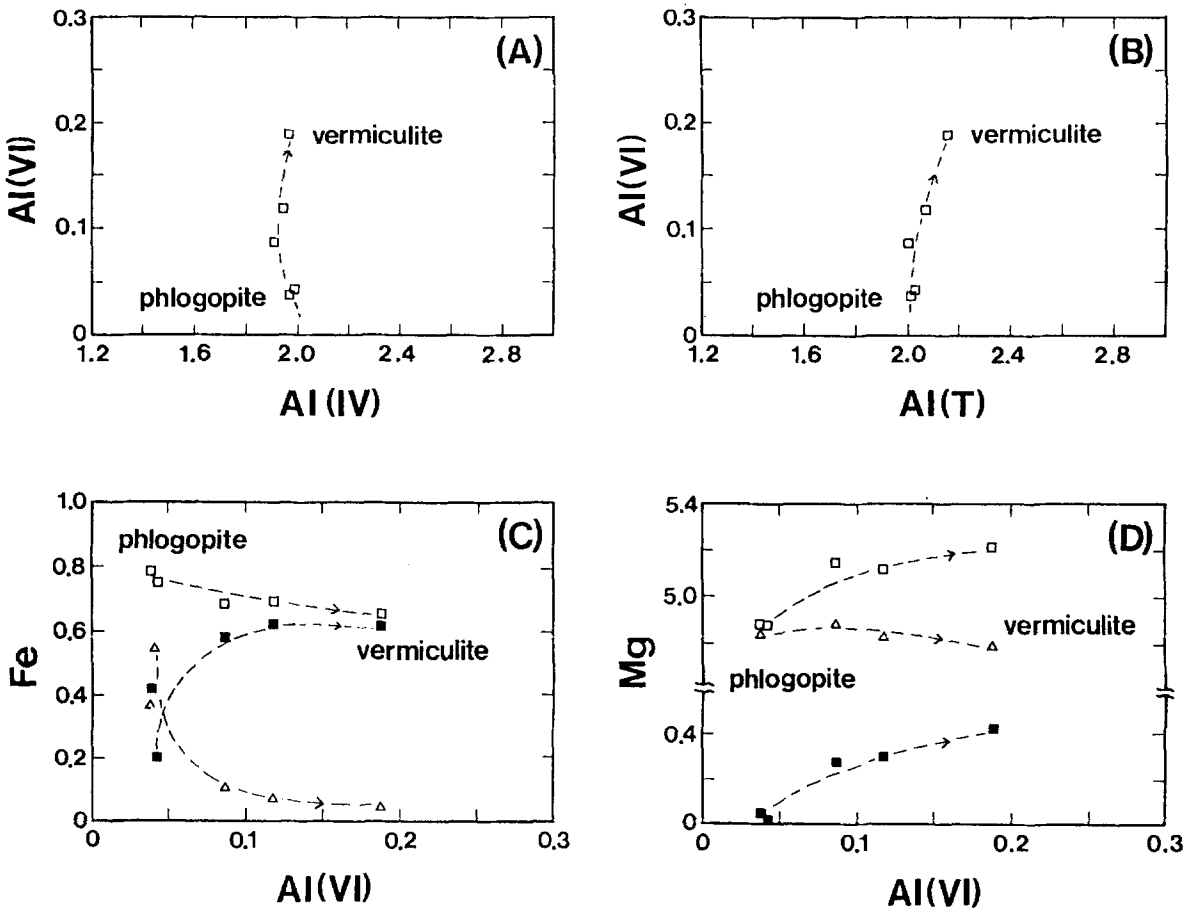

Figure 5. Compositional variations for phlogopite weathering to vermiculite: A) Al(IV) (tetrahedral Al) *vs.* Al(VI) (octahedral Al); B) Al(T) (total Al) *vs.* AL(VI); C) Al(VI) *vs.* Fe (open rectangle = Fe^{2+} + Fe^{3+}; solid rectangle = Fe^{3+}; and open triangle = Fe^{2+}); and D) Al(VI) *vs.* Mg (open rectangle = total Mg; open triangle = Mg in octahedral sites assuming there are 0.2 vacancies per unit cell in octahedral sites; and solid rectangle = Mg treated as interlayer cations, assuming there are 0.2 vacancies per unit cell in octahedral sites).

charge and can cause a surplus of positive charge in mica-like layers because of the excess amount of Fe. If all Fe is treated as ferric in vermiculite (solid rectangle in Figures 6A and 6B), the degree of Al-for-Si substitutions [Al(IV) is 3.24] is much higher than if all Fe occurs as ferrous [Al(IV) is 2.87; open rectangle in Figures 6A and 6B]. The increase of Al-for-Si tetrahedral substitutions can also be considered as the charge-compensation effect for the surplus of positive charge by the oxidation and enrichment of Fe in octahedral sites. The increase of Al substitutions for tetrahedral sites interferes with the Al substitutions for octahedral sites in spite of he increase of Al(T). If all Fe is calculated as ferric in vermiculitic phases (shown as a solid rectangle in Figure 6C), then the degree of these substitutions is much less than if all Fe were treated as ferrous (shown as an open rectangle in Figure 6C). The reason for the increase in Fe in the late stage of the vermiculitization of biotite is unknown and requires further study.

Consideration of structural formula for vermiculite

The status of Fe in vermiculite is a major factor controlling the substitutions in the 2:1 layer, especially vermiculites derived from biotites containing a relatively large amount of Fe. Furthermore, Mg contents in octahedral sites cannot be determined by electron microprobe analysis, which determines only total Mg contents. The structural formula of vermiculite must be recalculated (Table 3) on the basis of several assumptions. In the case of the vermiculites derived from phlogopite (P-1 in Table 1), the status of Fe had already been determined. The Mg contents in interlayer sites were then recalculated on the basis of two assumptions: a portion of the Mg content is treated as interlayer cations 1) until the layer charge reaches 1.2, which is the lower limit for vermiculite; or 2) until the sum of exchangeable cations reaches 150 meq/100 g (Table 3). These two recalculations yielded reasonable structural formulas indicating a significant amount of the Mg

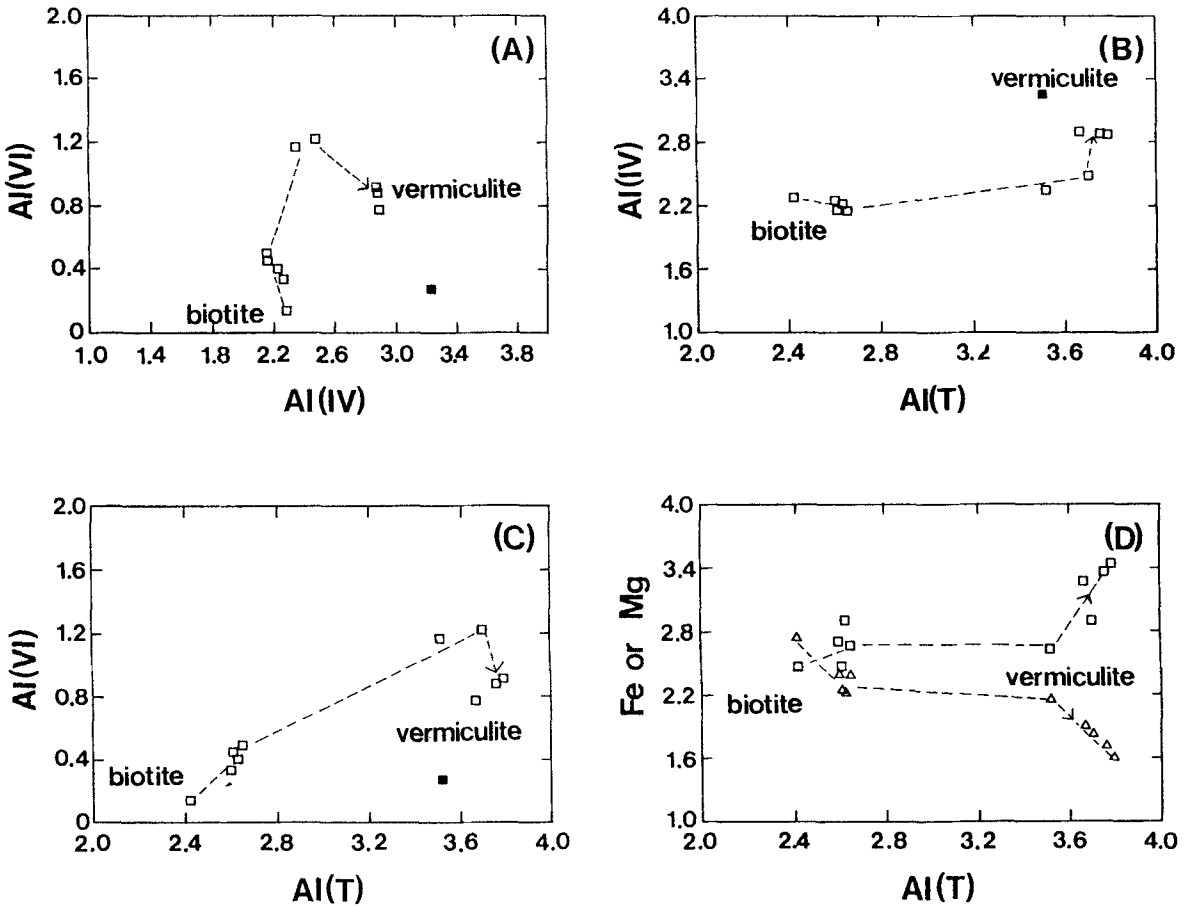

Figure 6. Compositional variations for biotite weathering to vermiculite: A) Al(IV) *vs.* Al(VI); B) Al(T) *vs.* Al(N); C) Al(T) *vs.* Al(VI), and D) Al(T) *vs.* Fe (open rectangle) and Mg (open triangle). The solid rectangle indicates the region of vermiculite, assuming all Fe is ferric.

must be in interlayer sites to form a reasonable vermiculite structure. The structural formula of Ca-saturated vermiculite (last column in Table 1, P-1Ca) shows that Mg in octahedral sites is 4.71, and total octahedral cations are 5.75. The formula indicates that the vacant sites in the octahedral position of vermiculite are ~0.25 per unit cell. It shows a reasonable agreement with the calculated value on the basis of the above assumptions.

The structural formula of vermiculite derived from biotite (B-1 in Table 2) was also recalculated on the basis of three assumptions: 1) all Fe is assumed to be in the ferrous state, and the Mg contents equal to the excess of cations in the octahedral sites are treated as interlayer cations; 2) all Fe is assumed to be in the ferric state, and if the sum of octahedral cations exceeds 6, the Mg contents equal to the excess of cations are treated as interlayer cations; and 3) all Fe is assumed to be in the ferric state, and a portion of the Mg content is treated as interlayer cations until the layer charge is equal to 1.2. The recalculated structural formulas based on the above three assumptions are listed in the right part of Table 3. Layer charges were calculated by the multiplication of cation numbers by the atomic charges of each element and the subtraction of the sum of them from a total negative charge of 44 [based on $O_{20}(OH)_4$ structual formula].

In the case of the first assumption (1), the calculated vermiculite formula exhibits a relatively high layer charge (1.91) and sum of exchangeable cations (184.43 meq/100 g). In fact, these values are much higher, supposing the vacancy in octahedral sites; therefore, assumption No. 1 is not reasonable. In the case of the second assumption (2), the calculation produces a substantial number of vacant sites (0.3 per unit cell). The layer charge and the sum of exchangeable cations are 0.36 and 37.06 (meq/100 g), respectively. These values are much lower than those of average vermiculite. In the case of the third assumption (3), the calculation yielded a reasonable formula, layer charge (1.20), and

Table 3. Calculated structural formulae for two representative vermiculites on the basis of several assumptions discussed in text.

Assumptions	Vermiculite from phlogopite		Vermiculite from biotite			
	1	2	1	2	3	4
Si	6.04	6.04	5.13	4.76	4.76	4.89
Al(IV)	1.96	1.96	2.87	3.24	3.24	3.11
Al (VI)	0.19	0.19	0.92	0.28	0.28	0.50
Ti	0.07	0.07	0.02	0.02	0.02	0.02
Cr	0.07	0.07	0.00	0.00	0.00	0.00
Fe^{3+}	0.62	0.62	0.00	3.19	3.19	2.10
Fe^{2+}	0.04	0.04	3.43	0.00	0.00	1.17
Mn	0.01	0.01	0.03	0.02	0.02	0.02
Ni	0.01	0.01	0.00	0.00	0.00	0.00
Mg	4.86	4.79	1.60	2.19	1.77	1.79
Σ(VI)	5.87	5.80	6.00	5.70	5.28	5.60
Mg	0.35	0.42	0.76	0.00	0.42	0.46
Ca	0.23	0.23	0.13	0.12	0.12	0.12
Na	0.00	0.00	0.02	0.02	0.02	0.02
K	0.04	0.04	0.11	0.10	0.10	0.10
Σ(interlayer cation)	0.62	0.69	1.02	0.24	0.66	0.70
L.C.[1]	1.20	1.34	1.91	0.36	1.20	1.28
	Calculated exchangeable cations (meq./100 g)					
Mg	78.20	93.86	147.37	0.00	88.32	92.94
Ca	51.50	51.50	24.61	24.61	24.61	24.61
Na	0.35	0.35	2.26	2.26	2.26	2.26
K	4.29	4.29	10.19	10.19	10.19	10.19
Σ(cation)	134.34	150.00	184.43	37.06	125.38	130.00

[1] Layer charges were calculated on the basis of $O_{20}(OH)_4$. Layer Charge = 44 (sum of multipling cation numbers by atomic charges of each element).

sum of exchangeable cations (125.38 meq/100 g). However, the octahedral sites exhibit excessive vacancies, 0.72 per unit cell.

The structural formula of vermiculite was recalculated on the basis of a fourth assumption (4), i.e., that the sum of exchangeable cations is 130 meq/100 g and the octahedral site vacancies are 0.4 on the basis of 22 oxygens because the vacant sites of biotite are more than those of phlogopite and generally known as 0.3 to 0.5 (Foster, 1960). Therefore, a part of the Mg contents is treated as interlayer cations until the sum of exchangeable cations reaches 130 meq/100 g and a part of the Fe contents is assumed to be in the ferric state until the octahedral vacant sites reach to 0.4.

The results are shown as the last column in Table 3. In this case, the vermiculite shows more reasonable structural formula, layer charge (1.28), and relatively high ferric Fe contents. These results indicate that a significant amount of Mg in both (two) vermiculites must be considered to be interlayer cations, and the vermiculite derived from biotite requires oxidation of at least a part of its ferrous Fe. This result suggests that vermiculitization from biotite probably occurs in the Si-deficient state. Therefore, it leads to greater substitution of Al for Si in tetrahedral sites, exceeding ~3 per unit cell, as shown on the right side of Table 3. Thus, charge compensation was achieved by replacement of divalent octahedral Fe by trivalent Fe by means of oxidation.

CONCLUSIONS

XRD and electron microprobe analyses suggest that the vermiculitization of mica results in the formation of regularly interstratified mica/vermiculite, which becomes increasingly enriched in the vermiculite component with increased weathering. The early stage of the vermiculitization of phlogopite proceeds by means of a continuous decrease of Al-for-Si tetrahedral substitutions and a progressive increase of Al-for-(Fe^{2+} + Mg) octahedral substitutions with weathering. These substitutions occur to compensate for the excess of negative charges in the mica-like layers. This vermiculitization process is in good agreement with currently accepted weathering mechanisms (e.g., Proust *et al.*, 1986; Fordham, 1990b, 1990c). In the late stage of the vermiculitization of phlogopite, these substitutions change to a slight increase of Al for Si in tetrahedral positions. This is likely the result of the oxidation of Fe, despite its small content. The early stage of the vermiculitization of biotite follows trends similar to that of phlogopite. It differs in the late stage of the transformation of biotite into vermiculite, however, in

that Al(IV) and Fe increase substantially. The late transformation stage is the one in which the enrichment and oxidation of Fe occur. The reason for the Fe enrichment in the late stage of the vermiculitization of biotite is not fully understood, but it must be partly responsible for the oxidation of Fe due to the weathering processes. Recalculations of the structural formulas of two vermiculites on the basis of several assumptions indicate a substantial amount of the Mg must be treated as interlayer cations. Additionally, the oxidation of Fe is required for the formation of vermiculite from biotite but is not always necessary for the formation of vermiculite from phlogopite.

ACKNOWLEDGMENTS

This research was supported by the Center for Mineral Resources, which is sponsored by Korea Science and Engineering Foundation, and partially by the Office of Environmental Restoration and Waste Management, U.S. Department of Energy, under contract DE-AC05-84OR21400 with Martin Marietta Energy Systems Inc., Environmental Sciences Division, Oak Ridge National Laboratory. The authors thank R. E. Ferrell Jr., Mike Timpson, Mark Elless, and R. April for their critical reviews and valuable comments.

REFERENCES

April, R. H., Hluchy, M. M., and Newton, R. M. (1986) The nature of vermiculite in Adirondack soils and till: *Clays & Clay Minerals* **34,** 549–556.

Bain, D. C., Mellor, A., and Wilson, M. J. (1990) Nature and origin of an aluminous vermiculitic weathering product in acid soil from upland and catchments in Scotland: *Clay Miner.* **25,** 467–475.

Banfield, J. F. and Eggleton, R. A. (1988) Transmission electron microscope study of biotite weathering: *Clays & Clay Minerals* **36,** 47–60.

Bence, A. E. and Albee, A. L. (1968) Empirical correction factors for the electron microanalysis of silicates and oxides: *J. Geol.* **76,** 382–403.

Coleman, N. T., Le Roux, F. H., and Cady, K. G. (1963) Biotite-hydrobiotite-vermiculite in soils: *Nature* **198,** 409–410.

Fordham, A. W. (1990a) Weathering of biotite into dioctahedral clay minerals: *Clay Miner.* **25,** 51–63.

Fordham, A. W. (1990b) Treatment of microanalyses of intimately mixed products of mica weathering: *Clays & Clay Minerals* **38,** 179–186.

Fordham, A. W. (1990c) Formation of trioctahedral illite from biotite in a soil profile over granite gneiss: *Clays & Clay Minerals* **38,** 187–195.

Foster, M. D. (1960) Interpretation of the composition of trioctahedral micas: *Geol. Survey Prof. Paper* **354-B,** 11–48.

Ildefonse P., Manceau, A., Proust, D., and Groke, M. C. T. (1986) Hydroxy-Cuvermiculite formed by the weathering of Fe-biotites at Salobo, Carajas, Brazil: *Clays & Clay Minerals* **34,** 338–345.

Kim, H. Y. (1992) Mineralogical and chemical study of the vermiculites in the weathering profile, in the Cheongyang area: MSc. thesis, Yonsei University, 57 pp. (unpublished, in Korean).

Kiss, E. (1967) Chemical determination of some major constituents in rocks and minerals: *Analy. Chim. Acta* **39,** 223–234.

MacKenzie, R. C. (1958) The evaluation of clay mineral composition with particular reference of smectites: *Silicates Industries* **25,** 12–18.

Meunier, A. and Velde, B. (1979) Biotite weathering in granites of western France: in *Proc. Int. Clay Conf., Oxford, 1978,* M. M. Mortland and V. C. Farmer, eds., Elsevier, Amsterdam, 405–415.

Newman, A. C. D. and Brown, G. (1987) The chemical constituent of clays: in *Chemistry of Clays and Clay Minerals,* Monograph No. 6, A. C. D. Newman, ed., Mineralogical Society, London, 1–128.

Proust, D., Eymery, J. P., and Beaufort, D. (1986) Supergene vermiculitization of a magnesian chlorite: Iron and magnesium removal processes: *Clays & Clay Minerals* **34,** 572–580.

Reynolds, R. C. (1980) Interstratified clay minerals: in *Crystal Structures of Clay Minerals and Their X-ray Identification,* G. W. Brindley and G. Brown, eds., Mineralogical Society, London, 249–303.

Rhoades, J. D. and Coleman, N. T. (1967) Interstratification in vermiculite and biotite produced by potassium sorption: I. Evaluation by X-ray diffraction pattern inspection: *Soil Sci. Soc. Amer. Proc.* **31,** 366–372.

Song, Y., Kwon, I. S., and Moon, H. S. (1990) Mineralogy of vermiculite occurring in the Cheongyang area: *J. Miner. Soc. Korea* **3,** 60 (in Korean).

(Received 27 April 1992; accepted 26 February 1994; Ms. 2217)